

# Finite-Element Analysis of Hepatic Multiple Probe Radio-Frequency Ablation

Dieter Haemmerich, *Student Member, IEEE*, Supan Tungjitkusolmun, *Member, IEEE*, S. Tyler Staelin, Fred T. Lee, Jr., David M. Mahvi, and John G. Webster\*, *Life Fellow, IEEE*

**Abstract**—Radio-frequency (RF) ablation is an important means of treatment of nonresectable primary and metastatic liver tumors. RF ablation, unlike cryoablation (a method of tumor destruction that utilizes cold rather than heat), must be performed with a single probe placed serially. The ablation of any but the smallest tumor requires the use of multiple overlapping treatment zones. We evaluated the performance of a configuration incorporating two hooked probes (RITA model 30). The probes were lined up along the same axis in parallel 20 mm apart. Three different modes applied voltage to the probes. The first mode applied energy in monopolar mode (current flows from both probes to a dispersive electrode). The second mode applied the energy to the probes in bipolar mode (current flows from one probe to the other). The third method applied the energy sequentially in monopolar mode (in 2-s intervals switched between the probes). We used the finite-element method (FEM) and analyzed the electric potential profile and the temperature distribution at the end of simulation of a 12-min ablation. The alternating monopolar mode allowed precise independent control of the amount of energy deposited at each probe. The bipolar mode created the highest temperature in the area between the probes in the configuration we examined. The monopolar mode showed the worst performance since the two probes in close vicinity create a disadvantageous electric field configuration. We, thus, conclude that alternating monopolar RF ablation is superior to the other two methods.

**Index Terms**—Ablation, bipolar ablation, electrode, finite-element model, hepatic ablation, liver ablation, radio-frequency ablation, RF ablation.

## I. INTRODUCTION

**R**ADIO-FREQUENCY (RF) ablation is increasingly utilized as a minimally invasive treatment for primary and metastatic liver tumors. Primary hepatocellular carcinoma is a significant worldwide public health problem with an estimated annual mortality of 1 000 000 [1]. Surgical resection offers the best chance of long-term survival, but is rarely possible. In

many patients with cirrhosis or multiple tumors hepatic reserve is inadequate to tolerate resection and alternative means of treatment that target the tumor, but preserve uninvolved liver are necessary [2]. In RF ablation, RF current is delivered to the tissue via electrodes inserted percutaneously or during surgical exploration. Different modes of controlling the electromagnetic power delivered to tissue can be utilized. Power-controlled mode ( $P = \text{constant}$ ), temperature-controlled mode ( $T = \text{constant}$ ) and impedance-controlled mode ( $Z < \text{constant}$ ) are used. Tumor cell death results from the conversion of electromagnetic energy to heat by ionic agitation. Temperatures above 45 °C–50 °C cause denaturation of intracellular proteins and destruction of membranes of tumor cells, eventually resulting in cell necrosis [3]. One of the major limitations of this technique is the inability to use multiple probes simultaneously. When tumors greater than 2 cm are treated, multiple applications are necessary to obtain complete tumor necrosis. Often tumor cells survive, which leads to high recurrence rates [4]–[6]. In cases where multiple tumors are present, these must be treated sequentially. Treatment time could be drastically reduced if multiple tumors could be treated simultaneously. Several methods have been investigated for increasing lesion size and improving efficacy. Internally cooled probes have been used [7], [8]. Pulsed techniques have been used to further increase necrosis diameter created by internally cooled probes [9]. Interstitial saline infusion creates larger lesions by cooling and increasing effective electrode area [10]–[12]. The cooling effects of large blood vessels and vascular perfusion can be minimized by clamping the hepatic artery and portal vein and occluding vascular inflow [13]. Inflow occlusion, however, requires a major surgical procedure, which negates one of the major advantages of RF ablation—the use in a minimally invasive fashion (percutaneous or laparoscopic). Bipolar RF ablation has been shown to create larger lesions using two needle electrodes compared with monopolar ablation using a single-needle electrode, when the two probes are placed close to each other [2], [12], [14], [18]. However, we have found no other studies investigating possible simultaneous usage of multiple ablation probes.

There have been many finite-element method (FEM) studies of cardiac RF ablation [15], [16] but only few FEM studies on hepatic ablation [17], [18]. We generated FEM models to analyze differences in distribution of temperature and electric field potential. We investigated the potential of three different modes that could be employed to allow the usage of multiple probes simultaneously. We placed two commonly used hooked electrodes (model 30, RITA Medical Systems, Mountain View, CA)

Manuscript received May 28, 2001; revised February 19, 2002. This work was supported by the National Institutes of Health (NIH) under Grant HL56143 and Grant DK58839. *Asterisk indicates corresponding author.*

D. Haemmerich, S. T. Staelin, and D. M. Mahvi are with the Department of Surgery, University of Wisconsin, Madison, WI 53792 USA.

S. Tungjitkusolmun is with the Department of Electronics, Faculty of Engineering, King Mongkut's Institute of Technology Ladkrabang, Ladkrabang, Bangkok 10520, Thailand.

S. T. Staelin and D. M. Mahvi are with the Department of Surgery, University of Wisconsin, Madison, WI 53792 USA.

F. T. Lee is with the Department of Radiology, University of Wisconsin, Madison, WI 53792 USA.

\*J. G. Webster is with the Department of Biomedical Engineering, University of Wisconsin, 1410 Engineering Drive, Madison, WI 53706 USA. (e-mail: webster@engr.wisc.edu).

Publisher Item Identifier 10.1109/TBME.2002.800790.

in parallel. The first mode applied energy in monopolar mode (current flows from both probes to a dispersive electrode). The second mode applied energy to the probes in bipolar mode (current flows from one probe to the other). The third mode applied energy sequentially in monopolar mode (in 2-s intervals current is switched either from one or the other probe to the dispersive electrode).

## II. METHODS

### A. The Bioheat Equation

RF ablation destroys tissue by converting electric energy into thermal energy. The current flows from the conductive probe through the tissue to a surface dispersive electrode. Tissue in close vicinity of the probe tip is heated by ionic agitation.

The heating of tissue during RF ablation is governed by the bioheat equation

$$\begin{aligned} \rho c \frac{\partial T}{\partial t} &= \nabla \cdot k \nabla T + \mathbf{J} \cdot \mathbf{E} - h_{bl}(T - T_{bl}) - Q_m \\ h_{bl} &= \rho_{bl} c_{bl} w_{bl} \end{aligned} \quad (1)$$

where  $\rho$  is the density ( $\text{kg}/\text{m}^3$ ),  $c$  is the specific heat ( $\text{J}/(\text{kg} \cdot \text{K})$ ), and  $k$  is the thermal conductivity ( $\text{W}/(\text{m} \cdot \text{K})$ ).  $J$  is the current density ( $\text{A}/\text{m}^2$ ) and  $E$  is the electric field intensity ( $\text{V}/\text{m}$ ).  $T_{bl}$  is the temperature of blood,  $\rho_{bl}$  is the blood density ( $\text{kg}/\text{m}^3$ ),  $c_{bl}$  is the specific heat of the blood ( $\text{J}/(\text{kg} \cdot \text{K})$ ), and  $w_{bl}$  is the blood perfusion ( $1/\text{s}$ ).  $h_{bl}$  is the convective heat transfer coefficient accounting for the blood perfusion.  $Q_m$  ( $\text{W}/\text{m}^3$ ) is the energy generated by metabolic processes and was neglected since it is small compared with the other terms [8].

In the Pennes model described in the bioheat equation, the energy exchange between blood and tissue is modeled as a nondirectional heat source. One major assumption is that the heat transfer related to perfusion between tissue and blood occurs in the capillary bed, which turned out not to be fully correct. The main thermal equilibrium process takes place in the precapillary or postcapillary vessels. Nevertheless, the Pennes model describes blood perfusion with acceptable accuracy, if no large vessels are nearby [20]. The blood perfusion in hepatic tissue used in the FEM was  $w_{bl} = 6.4 \times 10^{-3}$  [21].

### B. Finite-Element Analysis Software

We used PATRAN Version 9.0 (The MacNeal-Schwendler Co., Los Angeles, CA) to generate the geometric models, assign material properties, assign boundary conditions and perform meshing. After creating the model, PATRAN generates an input file for the ABAQUS/Standard 5.8 (Hibbitt, Karlsson & Sorensen, Inc., Pawtucket, RI) solver. A coupled thermo-electrical analysis was performed by ABAQUS. For postprocessing we used the built-in module ABAQUS/POST to generate profiles of temperature and electric field potential. All analysis was performed on a HP-C180 workstation equipped with 1.1 GB of RAM and 34 GB of hard disk space. Tungjitkusolmun *et al.* [15] provide a detailed description of the FEM modeling process.

### C. Model Geometry

Fig. 1 shows that we created FEM models of two RITA model 30, four-prong probes axially lined up in parallel. The probes

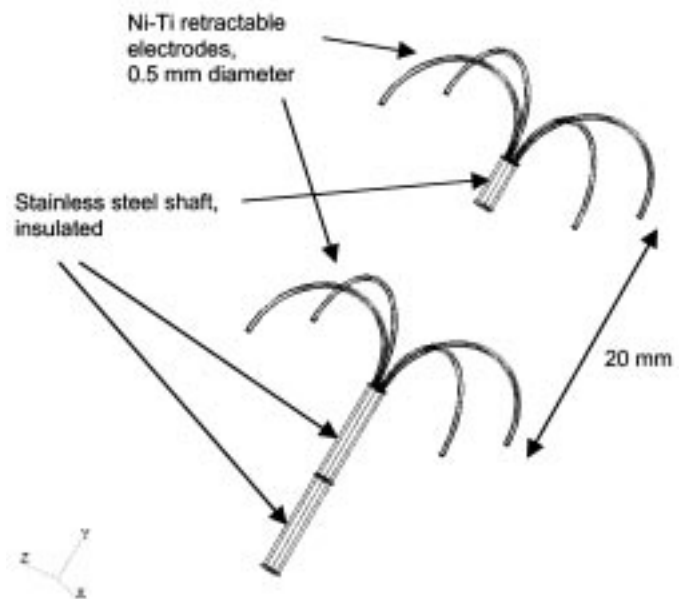


Fig. 1. Geometry of the probe arrangement used in the FEM. Only the prongs conduct RF current. The orientation of the coordinates is shown at the bottom.

have thermistors placed in each prong tip. In temperature-controlled mode the temperature sensed by the thermistors is used to control the applied power. The probes were placed 20 mm apart. An initial model with 25-mm separation did not produce a confluent lesion. In the actual probes, the prongs and the last 5 mm of the shaft are conducting. In our model only the prongs are conducting and the shaft is insulated. We insulated the shaft completely, because otherwise a disadvantageous current distribution would result when using the bipolar mode, as we described in more detail previously [18]. The shaft was insulated for all models to get comparable results. We placed the probes within an 80-mm diameter cylinder of liver tissue in this formation. Due to the symmetry of the arrangement, we could reduce computing time by modeling only a quarter of the cylinder. We used the same material properties as in previous models [18]. We set the initial temperature of the liver tissue and temperature at the boundary of the model to  $37^\circ\text{C}$ . We simulated ablation for 12 min. The model consisted of  $\sim 63\,000$  tetrahedral elements and  $\sim 12\,000$  nodes. We used a nonuniform mesh; mesh size was 0.2 mm close to the probe where we see large temperature and current gradients and 5 mm at the model boundaries. We performed convergence tests to ensure adequate spatial resolution. The time steps during the solution of the FEM started at 0.05 s and were subsequently automatically controlled by the solver software so that the maximum temperature change during the step was below  $3^\circ\text{C}$ .

### D. Energy Delivery Schemes for Multiple Probes

We used the same model geometry for all three types of energy delivery. Also, for all three types we controlled the applied energy (i.e., voltage) so that the tip temperature was kept at  $90^\circ\text{C}$  (temperature-controlled mode). We simulated ablation for 12 min.

The monopolar mode applied the same voltage to both probes. Current flows from the probe prongs to the disper-

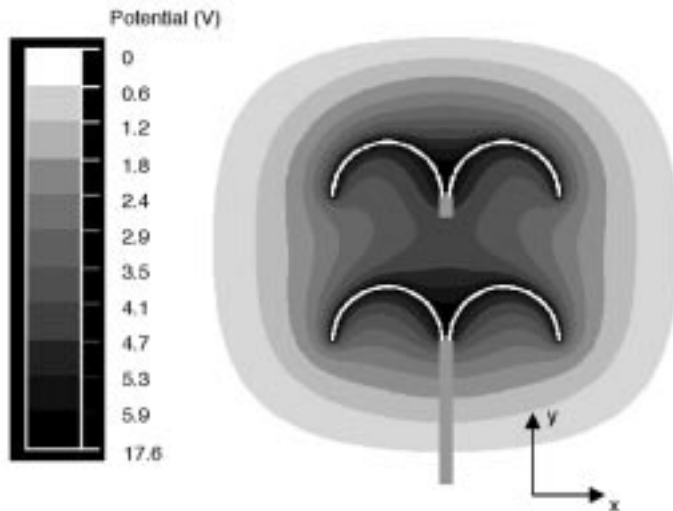


Fig. 2. Monopolar RF ablation Electric potential of FEM in the  $x$ - $y$  plane. The scale on the left shows potential in volts.

sive electrode. The bipolar mode passes current between the two probe prongs. We controlled the applied voltage so that the probe tips of the upper probe were kept at  $90\text{ }^{\circ}\text{C}$ . The upper probe tips get hotter because of the nonsymmetrical configuration of the two probes. The alternating monopolar scheme passed current from only one of the probe prongs to the dispersive electrode. After 2 s, the voltage alternately switches from the upper probe to the lower probe with all current collected by the dispersive electrode. The applied voltage is controlled independently for each of the two probes so that the average tip temperature of both probes is kept at  $90\text{ }^{\circ}\text{C}$  by independently controlling the applied voltage to each probe. The tip temperature is not constant in this case since one probe cools off while power is delivered to the other probe and vice versa. For monopolar mode and alternating monopolar mode, we assigned ground potential to the model boundaries.

### E. Model Limitations

Unlike our simplified FEM models, the liver is a very complex electrical and thermal organ due to its inhomogeneity. It is composed of three different types of blood vessels (hepatic arteries, portal veins, hepatic veins) of different diameters and flow velocities, liver parenchyma, hepatic tumors, bile ducts, and stroma, all of which have unique electrical and thermal properties. We did not include change of thermal and electrical tissue properties with temperature due to lack of data. Further, we considered perfusion to be homogenous and not dependent on temperature. These limitations of our model may lead to inaccurate results.

## III. RESULTS

For each of the three modes we show the temperature distribution in two planes at the end of the 12-min ablation period and the electric potential profile in the  $x$ - $y$  plane. We show the temperature distribution in the  $x$ - $y$  plane and in a plane of  $45^{\circ}$  offset to the  $x$ - $y$  plane. In all figures the probe tines are colored white and the probe stent is colored gray. For the monopolar mode, Fig. 2 shows the electric potential profile, Figs. 3 and 4 show the

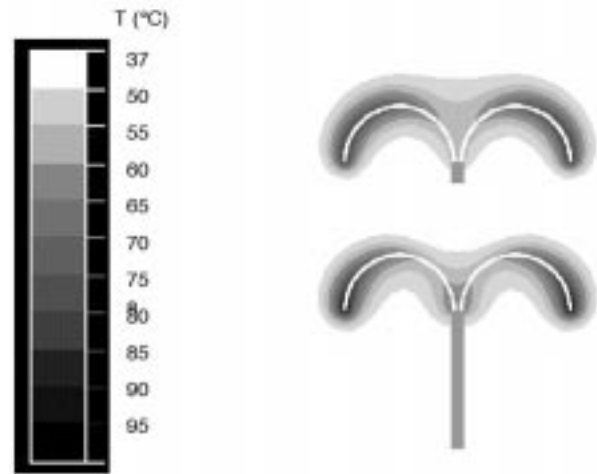


Fig. 3. Monopolar RF ablation. Temperature distribution in  $x$ - $y$  plane after 12-min RF ablation in temperature-controlled mode,  $T = 90\text{ }^{\circ}\text{C}$ . The outermost border (lightest gray) marks the  $50\text{ }^{\circ}\text{C}$  margin, which is considered the lesion border.

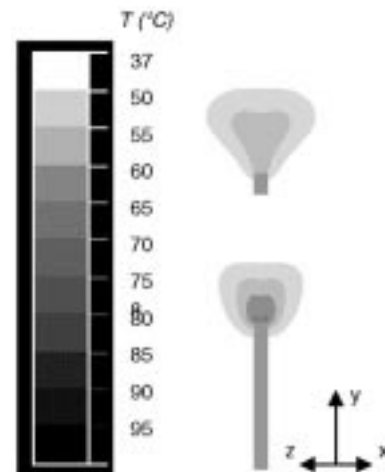


Fig. 4. Monopolar RF ablation. Temperature distribution in plane of  $45^{\circ}$  angle to  $x$ - $y$  plane after 12-min RF ablation in temperature-controlled mode,  $T = 90\text{ }^{\circ}\text{C}$ . The outermost border (lightest gray) marks the  $50\text{ }^{\circ}\text{C}$  margin, which is considered the lesion border.

temperature distributions. For the bipolar mode, Fig. 5 shows the electric potential profile and Figs. 6 and 7 show the temperature distribution. For the alternating monopolar mode, Fig. 8 shows the electric potential profile, Figs. 9 and 10 show the temperature distribution. Fig. 11 shows the progress of upper and lower tip temperatures for the alternating monopolar mode starting 11 min after start of ablation. The temperature range of the probe tips is  $79\text{ }^{\circ}\text{C}$ – $101\text{ }^{\circ}\text{C}$ . The temperature at the center between the two electrodes is  $42\text{ }^{\circ}\text{C}$  for the monopolar mode,  $56\text{ }^{\circ}\text{C}$  for the bipolar mode, and  $52\text{ }^{\circ}\text{C}$  for the alternating monopolar mode.

## IV. DISCUSSION

The aim of all three modes used in this study is to allow usage of multiple probes simultaneously while performing ablation. In the configuration we used in the FEM model, the probes are positioned 20 mm apart. This configuration is useful for treating large tumors, which cannot be treated with a single application

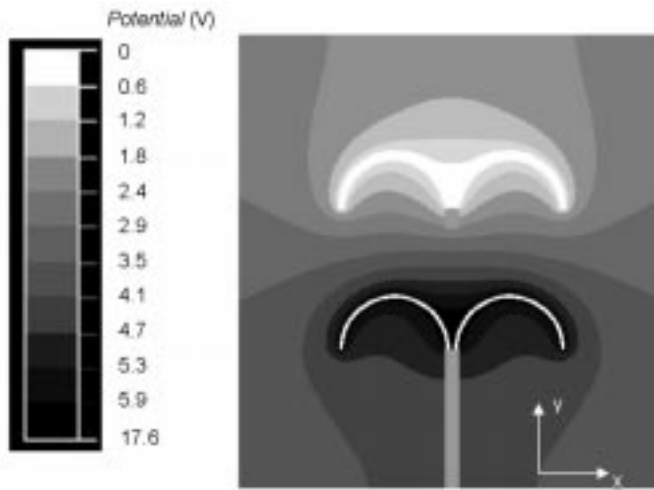


Fig. 5. Bipolar RF ablation. Electric potential of the FEM in the  $x-y$  plane. The scale on the left shows potential in volts.

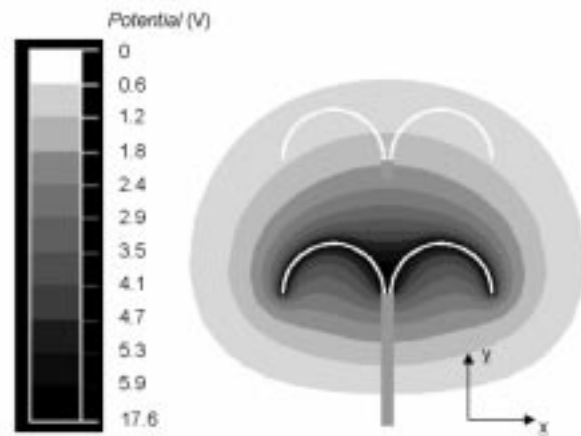


Fig. 8. Alternating monopolar RF ablation. Electric potential of the FEM in the  $x-y$  plane. The scale on the left shows potential in volts.

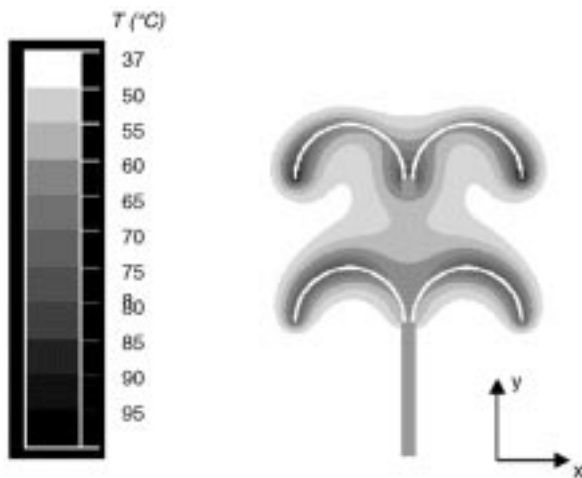


Fig. 6. Bipolar RF ablation. Temperature distribution in  $x-y$  plane after 12-min RF ablation in temperature-controlled mode,  $T = 90$  °C. The outermost border (lightest gray) marks the 50 °C margin, which is considered the lesion border.

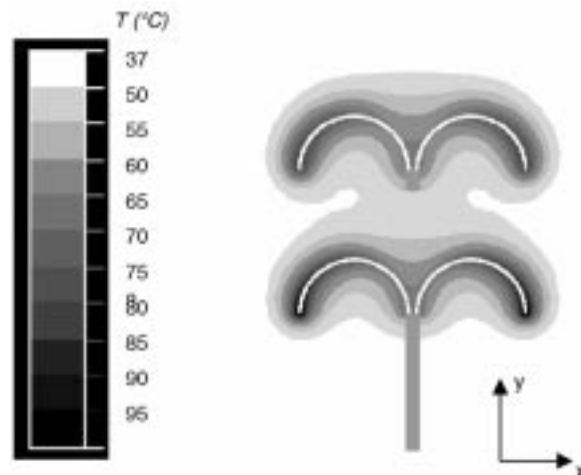


Fig. 9. Alternating monopolar RF ablation. Temperature distribution in  $x-y$  plane after 12-min RF ablation in temperature-controlled mode,  $T = 90$  °C. The outermost border (lightest gray) marks the 50 °C margin, which is considered the lesion border.

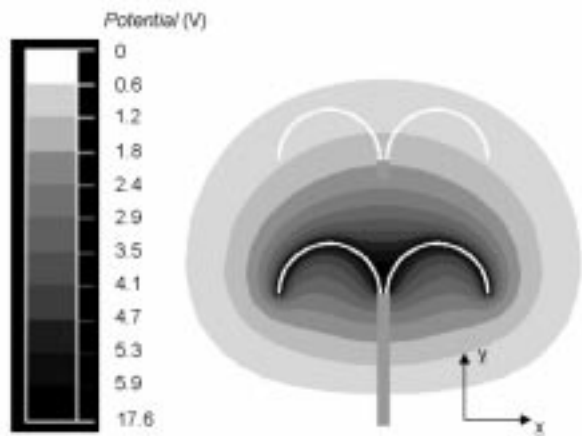


Fig. 7. Bipolar RF ablation. Temperature distribution in plane of  $45^\circ$  angle to  $x-y$  plane after 12-min RF ablation in temperature-controlled mode,  $T = 90$  °C. The outermost border (lightest gray) marks the 50 °C margin, which is considered the lesion border.

using a single probe. The configuration has an advantage based on a thermodynamic effect. If two lesions were created separately with electrodes at the same position as in a bipolar ablation, the total lesion size would be smaller than a single bipolar lesion. When only using a single probe, heat is diverted from the ablation site in all directions. When using two probes in close vicinity, one probe is thermally shielded by the opposing second probe, which also actively heats the tissue in its proximity. There is less cooling in the direction toward the collateral probe than would exist in monopolar ablation. Heat is trapped between the two probes and higher temperatures are reached. This results in a lesion of larger size than that of two lesions produced sequentially by ablation with probes placed at the same position. A zone of high temperature is created between the probes, which results in more effective killing of tumor cells in this zone.

However, the configuration of the probes is not limited to that in Fig. 1. With all three modes, probes can be placed further apart, as is necessary when treating multiple tumors. In the following sections we evaluate and compare the performance of each method.

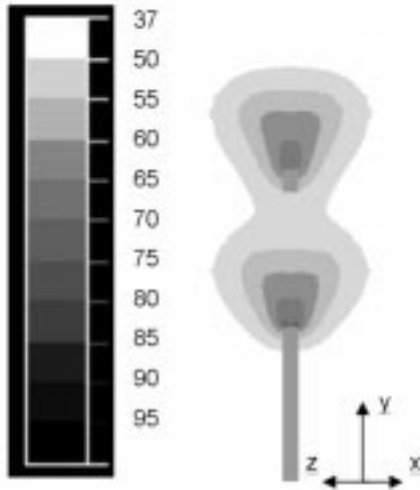


Fig. 10. Alternating monopolar RF ablation. Temperature distribution in plane of  $45^\circ$  angle to  $x$ - $y$  plane after 12-min RF ablation in temperature-controlled mode,  $T = 90^\circ\text{C}$ . The outermost border (lightest gray) marks the  $50^\circ\text{C}$  margin, which is considered the lesion border.

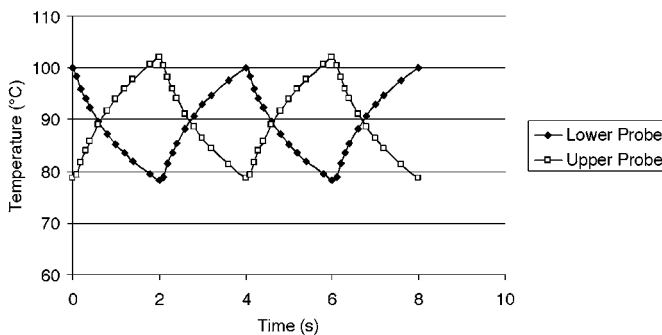


Fig. 11. Progress of upper and lower probe tip temperature during alternating monopolar ablation. The point  $t = 0$  corresponds to 11 min after start of ablation.

### A. Monopolar Mode

The main disadvantage of the monopolar mode is that current applied to both probes travels outward (toward a cutaneous dispersive electrode) with little traveling between them. Fig. 2 shows the electric potential created when the probes are placed close to each other. There is a large area of relatively constant electric potential between the two probes. The field gradient is small between the probes and there is reduced power deposition in this area. Figs. 3 and 4 show the temperature distribution. The temperature at the center in between the two probes is  $42^\circ\text{C}$  and far less than the temperature reached when using the bipolar or the alternating monopolar mode. This results in two separate lesions, whereas the other two modes create one confluent lesion. This effect is less pronounced when the probes are placed further apart. However, for a configuration where the probes are close to each other, this mode is not desirable. Another criteria for evaluating performance of the methods is the ease with which different amounts of energy can be deposited in the vicinity of each of the probes. The liver is a very heterogeneous and well-perfused organ. Significantly different conditions may exist in the vicinity of each of the probes. In RF

ablation, most of the active heating occurs in a range of a few millimeters from the electrodes. We can assume that similar resistivity and current density are present in the vicinity of both probes. Therefore, a comparable amount of energy is converted into heat next to each of the two probes, if we apply the same voltage. If one probe is cooled more by blood perfusion than the other due to differences in local perfusion next to each probe, more heat energy is carried away. One probe reaches a lower temperature than the other. The cooler probe then would have to carry a higher voltage than the other, so more energy is converted to heat in the vicinity of this probe. When two different voltages are applied to the two probes, current flows from each of the probes toward the dispersive electrode. Additionally current flows between the probes, which might also cause undesirable effects depending on the distance and voltage difference between the probes.

### B. Bipolar Mode

One way to solve the problem of the monopolar mode that arises from the disadvantageous electric field distribution is to use the bipolar mode. In the bipolar mode current passes between the two probes. Then no dispersive electrode is necessary. Fig. 5 shows the electric potential profile created using the bipolar mode. There are no areas of constant potential between the probes as occur when using the monopolar mode. More energy is converted to heat between the probes compared with the monopolar mode. Figs. 6 and 7 show the temperature distribution for the bipolar mode. The temperature at the center between the probes is  $56^\circ\text{C}$ . The bipolar mode is especially advantageous with the two probes in close proximity as we used in our simulation, since the current is more concentrated between the probes. The electric field gradient does not show large changes in the region between the probes. Tissue is preferentially heated in the region between the probes and reaches much higher temperatures than in the monopolar mode (Figs. 3 and 4). This advantage is not present when the two probes are placed far apart. When the probes are placed close to each other, the orientation of the probes relative to each other must be considered. If the probes are not placed symmetrically to a plane perpendicular to a plane that encompasses both of the probe axes, the sections of the probe that point toward the other probe will get hotter. Fig. 6 shows that the upper probe tips reach higher temperature compared with the lower probe tips. One disadvantage when using the bipolar mode is that only two probes can be used at the same time. For treating multiple tumors this means that only two tumors can be treated simultaneously. Another problem arises from the fact that all the current originating from one probe must also enter the second probe. We assume similar resistivity and current density in the vicinity of both probes, as for the monopolar mode. Then there is a comparable amount of electric energy converted to heat in the vicinity of both probes. When there is different amount of cooling at the location of each of the probes due to differences in perfusion, one probe reaches a lower temperature than the other. When using the bipolar scheme there is no way to independently control the amounts of heat generated in the vicinity of each of the probes.

### C. Alternating Monopolar Mode

The alternating monopolar mode solves most problems present in the two other modes. At one instant in time current flows from only one of the probes toward the dispersive electrode. The probe from which the current flows to the dispersive electrode is changed after 2 s. So the applied voltage alternates between the two probes at 2-s intervals. Fig. 11 shows the progress of tip temperatures of the upper and lower probe after equilibrium is reached ( $t = 0$  corresponds to 11 min after start of the ablation). During the 2-s interval we used, the tip temperature varies between 78 °C and 103 °C. Since tighter control of temperature is desirable, ideally a lower interval should be used (e.g., 0.5 s). However, with shorter intervals the amount of time a FEM simulation takes to run increases. We used the 2-s interval as a compromise. The alternating monopolar mode can be extended to more than two probes, so there is no theoretical limit on how many probes to use. Different amount of energy can be converted to heat at each of the probes easily by applying different voltages to the probes. In the bipolar mode, this is not possible. Also in the monopolar mode, this can only be done with limitations. Another way to deposit different amounts of energy to each of the probes is not to apply different voltages, but to apply the same voltage for different time intervals to each of the probes.

Fig. 8 shows the electric potential during the interval when voltage is applied to the lower probe. Since voltage is only applied to one of the probes, the probes do not interfere with each other as is the case for the monopolar mode. However, in a configuration where the probes are close to each other, the bipolar mode is advantageous due to the concentration of current in between the probes. In the bipolar mode the electric field gradient does not drop as sharply as in the alternating monopolar mode and also stays fairly constant in the region between the probes. This advantage also becomes apparent when comparing the temperature distributions of the alternating monopolar and the bipolar modes. Figs. 9 and 10 show that the temperature distribution of the alternating monopolar mode yields lower temperatures than the bipolar mode (Figs. 6 and 7). However, the alternating monopolar mode still shows significantly better results than the monopolar mode (Figs. 3 and 4), reaching a temperature of 52 °C at the center between the probes.

This advantage of the bipolar mode over the alternating monopolar mode is much less pronounced when the probes are moved far away from each other. Then the current distribution more closely matches that of the alternating monopolar mode.

### V. CONCLUSION

The alternating monopolar mode is the only mode where we can easily control the heat deposited at each probe. For treatment of multiple tumors with multiple probes, this mode is the most suitable. When probes are placed close to each other (e.g., to treat a large tumor), the bipolar mode creates the highest temperatures in the region between the two probes, but is limited to the use of two probes simultaneously. The monopolar mode is the most disadvantageous one of the three modes.

### REFERENCES

- [1] M. C. Kew, "The development of hepatocellular carcinoma in humans," *Cancer Surv.*, vol. 5, pp. 719–739, 1985.
- [2] S. A. Curley, B. S. Davidson, R. Y. Fleming, F. Izzo, L. C. Stephens, P. Tinkey, and D. Cromeens, "Laparoscopically guided bipolar radiofrequency ablation of areas of porcine liver," *Surg. Endosc.*, vol. 11, pp. 729–733, 1997.
- [3] W. Lounsbury, V. Goldschmidt, and C. Linke, "The early histologic changes following electrocoagulation," *Gastrointest. Endosc.*, vol. 41, pp. 68–70, 1995.
- [4] S. Rossi, M. Di Stasi, E. Buscarini, P. Quaretti, F. Garbagnati, L. Squasante, C. T. Paties, D. E. Silverman, and L. Buscarini, "Percutaneous RF interstitial thermal ablation in the treatment of hepatic cancer," *Amer. J. Roentgenol.*, vol. 167, pp. 759–768, 1996.
- [5] L. R. Jiao, P. D. Hansen, R. Havlik, R. R. Mistry, M. Pignatelli, and N. Habib, "Clinical short-term results of radiofrequency ablation in primary and secondary liver tumors," *Amer. J. Surg.*, vol. 177, pp. 303–306, 1999.
- [6] L. Solbiati, T. Ierace, S. N. Goldberg, S. Sironi, T. Livraghi, R. Fiocca, G. Servadio, G. Rizzatto, P. R. Mueller, A. Del Maschio, and G. S. Gazelle, "Percutaneous US-guided radiofrequency tissue ablation of liver metastases: Treatment and follow-up in 16 patients," *Radiology*, vol. 202, pp. 195–203, 1997.
- [7] S. N. Goldberg, G. S. Gazelle, L. Solbiati, W. J. Rittman, and P. R. Mueller, "Radio-frequency tissue ablation: Increased lesion diameter with a perfusion electrode," *Acad. Radiol.*, vol. 3, pp. 636–644, 1996.
- [8] T. A. Lorentzen, "A cooled needle electrode for radio-frequency tissue ablation: Thermodynamic aspects of improved performance compared with conventional needle design," *Acad. Radiol.*, vol. 3, pp. 556–563, 1996.
- [9] S. N. Goldberg, M. C. Stein, G. S. Gazelle, R. G. Sheiman, J. B. Kruskal, and M. E. Clouse, "Percutaneous radiofrequency tissue ablation: Optimization of pulsed-radiofrequency technique to increase coagulation necrosis," *J. Vasc. Interv. Radiol.*, vol. 10, pp. 907–916, 1999.
- [10] Y. Miao, Y. Ni, S. Mulier, K. Wang, M. F. Hoes, P. Mulier, F. Penninckx, J. Yu, I. De Scheerder, A. L. Baert, and G. Marchal, "Ex vivo experiment on radiofrequency liver ablation with saline infusion through a screw-tip cannulated electrode," *J. Surg. Res.*, vol. 71, pp. 18–26, 1997.
- [11] R. S. Mittleman, S. K. Huang, W. T. De Guzman, H. Cuenoud, A. B. Wagshal, and L. A. Pires, "Use of saline infusion electrode catheter for improved energy delivery and increased lesion size in radiofrequency catheter ablation," *PACE*, vol. 18, pp. 1022–1027, 1995.
- [12] F. Burdio, A. Guemes, J. M. Burdio, T. Castiella, M. A. De Gregorio, R. Lozano, and T. Livraghi, "Hepatic lesion ablation with bipolar saline-enhanced radiofrequency in the audible spectrum," *Acad. Radiol.*, vol. 6, pp. 680–686, 1999.
- [13] E. Delva, Y. Camus, and B. Nordlinger, "Vascular occlusions for liver resections," *Ann. Surg.*, vol. 209, pp. 297–304, 1989.
- [14] J. P. McGahan, W.-Z. Gu, J. M. Brock, H. Tesluk, and C. D. Jones, "Hepatic ablation using bipolar radiofrequency electrocautery," *Acad. Radiol.*, vol. 3, pp. 418–422, 1996.
- [15] S. Tungjitkusolmun, E. J. Woo, H. Cao, J.-Z. Tsai, V. R. Vorperian, and J. G. Webster, "Thermal-electrical finite-element modeling for radio-frequency cardiac ablation: Effects of changes in myocardial properties," *Med. Biol. Eng. Comput.*, vol. 38, pp. 562–568, Sept. 2000.
- [16] —, "Finite-element analyzes of uniform current density electrodes for radio-frequency cardiac ablation," *IEEE Trans. Biomed. Eng.*, vol. 47, pp. 32–40, Jan. 2000.
- [17] M. G. Curley and P. S. Hamilton, "Creation of large thermal lesions in liver using saline-enhanced RF ablation," in *Proc. 19th Annu. Int. Conf. IEEE Eng. Med. Biol. Soc.*, Chicago, IL, 1997, pp. 2516–2519.
- [18] D. Haemmerich, S. T. Staelin, S. Tungjitkusolmun, F. T. Lee Jr., D. M. Mahvi, and J. G. Webster, "Hepatic bipolar radio-frequency ablation between separated multiprong electrodes," *IEEE Trans. Biomed. Eng.*, vol. 48, pp. 1145–1152, Oct. 2001.
- [19] S. Tungjitkusolmun, S. T. Staelin, D. Haemmerich, H. Cao, J.-Z. Tsai, H. Cao, J. G. Webster, F. T. Lee Jr., D. M. Mahvi, and V. R. Vorperian, "Three-dimensional finite-element analyzes for radio-frequency hepatic tumor ablation," *IEEE Trans. Biomed. Eng.*, vol. 49, pp. 3–9, Jan. 2002.
- [20] H. Arkin, L. X. Xu, and K. R. Holmes, "Recent developments in modeling heat transfer in blood perfused tissues," *IEEE Trans. Biomed. Eng.*, vol. 41, pp. 97–107, Feb. 1994.
- [21] E. S. Ebbini, S.-I. Umemura, M. Ibbini, and C. A. Cain, "A cylindrical-section ultrasound phased-array applicator for hyperthermia cancer therapy," *IEEE Trans. Biomed. Eng.*, vol. 35, pp. 561–572, 1988.



**Dieter Haemmerich** (S'00) was born in Vienna, Austria on May 22, 1971. He received the M.S. degree from the Department of Electrical and Computer Engineering, Technical University of Vienna, Vienna, Austria, in 2000, and the M.S. and Ph.D. degrees from the Department of Biomedical Engineering, University of Wisconsin, Madison, in 2000 and 2001, respectively.

He is currently an Assistant Scientist in the Department of Surgery, University of Wisconsin. His research interests include finite-element analysis of

radio-frequency ablation and tissue impedance measurement.



**Supan Tungjitsolmun** (S'96-M'00) was born in Bangkok, Thailand, December 5, 1972. He received the B.S.E.E. degree from the University of Pennsylvania, Philadelphia, in 1995, and the M.S.E.E. and Ph.D. degrees from the University of Wisconsin, Madison, in 1996, and 2000.

He is on the faculty of the Department of Electronics, Faculty of Engineering, and the Research Center for Communications and Information Technology, King Mongkut's Institute of Technology Ladkrabang, Bangkok, Thailand. His research

interests include finite-element modeling, radio-frequency cardiac ablation, and hepatic ablation.

He is a member of Tau Beta Pi, Eta Kappa Nu, and Pi Mu Epsilon.



**S. Tyler Staelin** attended the University of Michigan, Ann Arbor, and Vanderbilt University School of Medicine, Nashville, TN, prior to training in surgery at the University of Wisconsin Hospital and Clinics, Madison.

He is Chief Resident in Surgery at the University of Wisconsin Hospital and Clinics.



**Fred T. Lee, Jr.** received the BA and M.D. degrees from Boston University, Boston, MA, in 1984 and 1986, respectively.

After serving a residency in diagnostic radiology at The University of Rochester, Rochester, N.Y., he became a Faculty Member at the University of Wisconsin, Madison. He has been the Director of Abdominal Radiology since 2000. His research interests are in tumor ablation and radiographic contrast materials for the detection of cancer.



**David M. Mahvi** received the B.S. degree in microbiology and premed from the University of Oklahoma, Norman, in 1977 and the M.D. degree from the University of South Carolina, Columbia, in 1981. He then completed the following postgraduate medical clinical training programs at Duke University, Durham, NC: residency in surgery from 1981-1983; fellowship in immunology 1983-1985; residency in surgery 1985-1989.

In 1989, he joined the Section of Surgical Oncology, Department of Surgery at the University of Wisconsin-Madison where he is Professor of Surgery. He is Staff Surgeon, Oncologic and General Surgery, Middleton Memorial Veterans Hospital, Madison, WI and Member, University of Wisconsin Comprehensive Cancer Center.



**John G. Webster** (M'59-SM'69-F'86-LF'97) received the B.E.E. degree from Cornell University, Ithaca, NY, in 1953, and the M.S.E.E. and Ph.D. degrees from the University of Rochester, Rochester, NY, in 1965 and 1967, respectively.

He is Professor of Biomedical Engineering at the University of Wisconsin-Madison. In the field of medical instrumentation, he teaches undergraduate and graduate courses, and does research on radio-frequency cardiac and hepatic ablation.

Dr. Webster is editor of *Medical Instrumentation: Application and Design*, 3rd ed. (New York: Wiley, 1998), *Encyclopedia of Electrical and Electronics Engineering* (New York: Wiley, 1999), and *Minimally Invasive Medical Technology* (Bristol, U.K.: IOP Publishing, 2001). He is the recipient of the 2001 EMBS Career Achievement Award.